

Enzyme Activity

International Edition: DOI: 10.1002/anie.201712757

German Edition: DOI: 10.1002/ange.201712757

Modifying the Steric Properties in the Second Coordination Sphere of Designed Peptides Leads to Enhancement of Nitrite Reductase Activity

Karl J. Koebeke, Fangting Yu, Elvin Salerno, Casey Van Stappen, Alison G. Tebo, James E. Penner-Hahn, and Vincent L. Pecoraro*

Abstract: Protein design is a useful strategy to interrogate the protein structure-function relationship. We demonstrate using a highly modular 3-stranded coiled coil (TRI-peptide system) that a functional type 2 copper center exhibiting copper nitrite reductase (NiR) activity exhibits the highest homogeneous catalytic efficiency under aqueous conditions for the reduction of nitrite to NO and H₂O. Modification of the amino acids in the second coordination sphere of the copper center increases the nitrite reductase activity up to 75-fold compared to previously reported systems. We find also that steric bulk can be used to enforce a three-coordinate Cu^I in a site, which tends toward two-coordination with decreased steric bulk. This study demonstrates the importance of the second coordination sphere environment both for controlling metal-center ligation and enhancing the catalytic efficiency of metalloenzymes and their analogues.

De novo protein design is a powerful tool to assess the concept that biological function is a direct consequence of structure^[1–3] and to probe evolutionary conversion of one activity into another. One example is the insertion of functional carbonic anhydrase and nitrite reductase active sites into alpha-helical 3-stranded-coiled-coil (3SCC) scaffolds. These constructs provide protein folds that are completely unrelated to that of the native enzymes while retaining the core features of the catalytic metal-binding site.^[4–6] Furthermore, studies have revealed how proteins containing identical primary sequences and three-dimensional structures can be easily converted from hydrolytic into redox enzymes by the simple expedient of exchanging Zn^{II} by Cu^{II}. These advances have utilized the TRI family of peptides which are designed with a heptad repeat strategy to form 3SCCs.^[7] Hydrophobic amino acids that make up the 3SCC interior can be substituted to create transition-metal-binding sites while maintaining the overall fold of the structure. This strategy has successfully produced both a Zn-binding carbonic anhydrase mimic with activity that approaches that of the native

system, as well as a Cu-binding nitrite reductase (CuNiR) mimic.^[8] Other successful non-heme redox active de novo constructs include the Due Ferri system^[9,10] and 4Fe–4S clusters.^[11,12]

Copper proteins play important roles in many biological processes.^[13,14] Type 2 copper (T2Cu) centers are mononuclear Cu^{II}(His)_n(X)_{4–n} metal-binding sites that serve various functions in native proteins.^[14] CuNiR, which carries out the dissimilatory reduction of NO₂[–] to NO, contains a T2Cu catalytic center [Cu^I(His)₅(OH₂)]. We have previously described a structural and functional model for the CuNiR T2Cu center using a TRI peptide derivative capable of catalyzing nitrite reduction at a rate of 5 turnovers over the course of 3.7 hours.^[6,15] Despite exhibiting similar reactivity, this activity is seven orders of magnitude below that of comparable natural CuNiRs. This may be due to the difficulty of incorporating non-heme redox centers into de novo scaffolds, in which one must consider the preferred coordination of both Cu oxidation states in the catalytic cycle. In this first generation model we have shown Cu^I to exist in a three-coordinate state, the same coordination number as the native, ascorbate-reduced T2Cu center in CuNiR.^[16] Based on EPR spectroscopy, the oxidized form of this designed protein likely binds to Cu^{II} with a higher coordination number (five coordinate) than is seen in the native form of oxidized CuNiR (four coordinate). The de novo construct also possessed a higher reduction potential than native CuNiR, suggesting significant deviation from native CuNiR redox behavior. To address how these factors influence reactivity, we carried out stepwise modifications of the helical interface to create a series of peptides with reduction potentials spanning approximately 200 mV and NiR reaction rates that varied by a factor of four.^[15] Exploiting remote interactions, we were able to successfully alter copper-binding affinities, reduction potentials, and protonation equilibria.

We now turn our attention to the interior of the coiled coils to examine the impact of changes in the second coordination sphere. Our initial aim was to evaluate how steric constraints of the hydrophobic side chains around the metal center (either above or below) influence NiR activity. Previous studies comparing the coordination number of Cd^{II} bound in TRI systems revealed that while a mixture of CdS₃ and CdS₃O species were formed in Cd(TRIL16C)₃[–], only CdS₃O was obtained in Cd(TRIL12AL16C)₃[–] or Cd-(TRL16_DC)₃[–].^[17,18] Furthermore, the introduction of greater steric encumbrance in the Cd(TRIL12_DLL16C)₃[–] construct resulted in exclusive CdS₃ while providing greater proximal

[*] Dr. K. J. Koebeke, Dr. F. Yu, E. Salerno, C. Van Stappen, Dr. A. G. Tebo, Prof. J. E. Penner-Hahn, Prof. V. L. Pecoraro
Department of Chemistry
University of Michigan
Ann Arbor, MI 48109 (USA)
E-mail: vlpec@umich.edu

Supporting information and the ORCID identification number(s) for the author(s) of this article can be found under:
<https://doi.org/10.1002/anie.201712757>.

space to the metal-binding site in $\text{Cd}(\text{GRCSL16CL19}_D\text{L})_3^-$ led to the formation of CdS_3O_2 .^[19] These studies demonstrated that modification of steric bulk around the metal-binding site could control solvent/substrate access to the metal. The first generation CuNiR model peptide, **TRIW-H**, contains a Leu residue at the *d*-sites^[20] above and below the Cu-binding histidines in the 23rd position, in a fashion analogous to TRIL16C. Therefore, we substituted the Leu residues at the 19th and 26th positions in three different ways. First, we incorporated residues (Ile and D-Leu) that would be more sterically crowding around the metal center. Second, we replaced Leu with a less sterically demanding Ala residue that might enhance substrate access or allow greater conformational flexibility of the active site. Crystal structures of similar constructs ($\text{Hg}(\text{GRAND-CSL12AL16C})_3^-$ and $\text{Zn}(\text{GRAND-CSL12AL16C})_3^-$) show that the pocket created by substituting a Leu₃ layer for Ala₃ residues allows up to 4 molecules of water within the 3SCC interior near the metal-binding site.^[21,22] Third, we incorporated a potentially hydrogen-bonding ligand (Asp) that might assist in catalysis (Figure 1; Table 1). These modifications were predicted to impact the primary coordination sphere of the copper center and in turn modify NiR reactivity.

The NiR activities (pseudo-first order rate constants) of these peptides were measured following previously reported procedures.^[6] L19I and L19_DL variants showed no notable rate enhancement compared to the parent **TRIW-H**. Variants of **TRIW-H** with substitution of L19 or L26 with Ala had a marked increase in NiR rates compared to the parent from $4.6 \times 10^{-4} \text{ s}^{-1}$ for **TRIW-H** to $3.5 \times 10^{-2} \text{ s}^{-1}$ for L19A or $2.2 \times 10^{-2} \text{ s}^{-1}$ for L26A. Variants with L19 or L26 mutated to Asp had similarly enhanced rates from $4.6 \times 10^{-4} \text{ s}^{-1}$ for **TRIW-H** to $2.4 \times 10^{-2} \text{ s}^{-1}$ for L19D or $3.5 \times 10^{-2} \text{ s}^{-1}$ for L26D

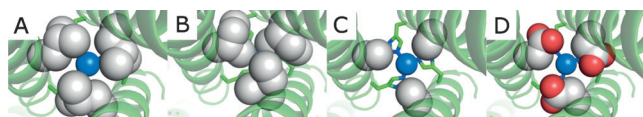


Figure 1. PyMol models of **TRIW-H** A) L19I, B) L19A, C) L19A, and D) L19D showing the change of steric packing above the copper center made based on the crystal structure of $\text{Zn}^{\text{II}}_{\text{N}}\text{Hg}^{\text{II}}_{\text{S}}(\text{CSL9PenL23H})_3^+$ (PDB code: 3PBJ) or $\text{Zn}^{\text{II}}(\text{H}_2\text{O})(\text{GRAND-CSL12AL16C})_3^-$ (5KB2). Peptide strands are represented by helices and His23 side chains are represented by sticks. Residues on the 19th position and Cu^{I} are shown in spheres to illustrate the space-filling above the copper center; Cu blue, O red.

Table 1: TRI family peptide sequences used in this study.

Peptides ^[a]	1	2	9	16 19	23	30
		abcdefg	abcdefg	Abcdefg	abcdefg	
TRIW-H	G	WKALEEK	LKALEEK	LKALEEK	HKALEEK	G
L19I	G	WKALEEK	LKALEEK	LKAIEEK	HKALEEK	G
L19 _D L	G	WKALEEK	LKALEEK	LKA _D LEEK	HKALEEK	G
L19A	G	WKALEEK	LKALEEK	LKAAEEK	HKALEEK	G
L26A	G	WKALEEK	LKALEEK	LKALEEK	HKAAEEK	G
L19D	G	WKALEEK	LKALEEK	LKADEEK	HKALEEK	G
L26D	G	WKALEEK	LKALEEK	LKALEEK	HKADEEK	G

[a] The C- and N-termini are amidated and acetylated, respectively.

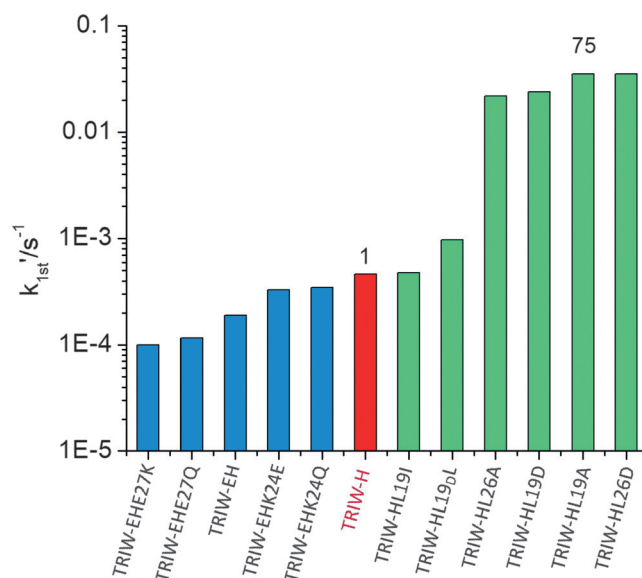


Figure 2. Pseudo-first order rate constants at pH 5.8 for the original construct **TRIW-H** (red), previously reported exterior mutations (blue), and currently reported interior mutations (green).^[15]

(Figure 2). Our study shows no evidence of additional catalytic enhancement from the use of protonated side chains compared to Ala. Yamaguchi and co-workers have previously reported a copper nitrite reductase model system $[\text{CuMe}_2\text{bpa}(\text{H}_2\text{O})(\text{ClO}_4)]^+$ (Me_2bpa : bis(6-methyl 2-pyridylmethyl)amine) which, when attached to an electrode surface, has a catalytic efficiency of $57 \text{ s}^{-1}\text{M}^{-1}$.^[23] However, based on the difference in the turnover number at pH 5.5 provided in their report, the catalytic efficiency, under homogeneous aqueous conditions, is estimated to be reduced to $2.2 \times 10^{-2} \text{ s}^{-1}\text{M}^{-1}$. Therefore, our **TRIW-H** L19A system has, thus far, the highest reported catalytic efficiency of an NiR model under homogeneous aqueous conditions at $1.0(0.3) \text{ s}^{-1}\text{M}^{-1}$ at pH 5.8 as determined by Michaelis–Menton kinetics (see Supporting Information).

Under catalytic conditions, the oxidized $\text{Cu}^{\text{II}}(3\text{SCC})$ is rapidly reduced by ascorbate to $\text{Cu}^{\text{I}}(3\text{SCC})$, followed by the slow re-oxidation of Cu^{I} into Cu^{II} coupled to nitrite reduction.^[6] Therefore, changes in the catalytic rate induced by secondary coordination sphere modifications could be the result of alterations in the nitrite interactions with the Cu^{I} “resting” state. For this reason, we examined the structure of the Cu^{I} center in the second-sphere-**TRIW-H** variants and compared them to the parent **TRIW-H** by X-ray absorption spectroscopy (XAS).

Previously, we have shown that Cu^{I} -bound **TRIW-H** was best described as a three coordinate Cu^{I} with 1.93 \AA Cu–N bond lengths at both pH 7.4 and pH 5.8.^[6] The XANES region of Cu^{I} contains an edge feature corresponding to the $1s \rightarrow 4p$ transition, whose relative intensity serves as a useful diagnostic of the coordination of Cu^{I} . As the coordination number of Cu^{I} increases, the degree of $4s\text{--}4p$ mixing increases as well, resulting in a greater degree of parity forbidden $1s \rightarrow 4s$ character and a decrease in intensity for this edge feature.^[24] Intensity ratios near 1:1 of this edge feature relative to the

edge jump are indicative of two-coordinate Cu^{I} , while a decrease to around 1:2 is typical of three-coordinate, and less than 1:2 of four-coordinate.^[25] Figure 3 demonstrates that the L19A and L19D constructs have a significantly more intense edge feature compared to the parent construct TRIW-H, or L19I and L19_DL, consistent with a two-coordinate Cu^{I} .

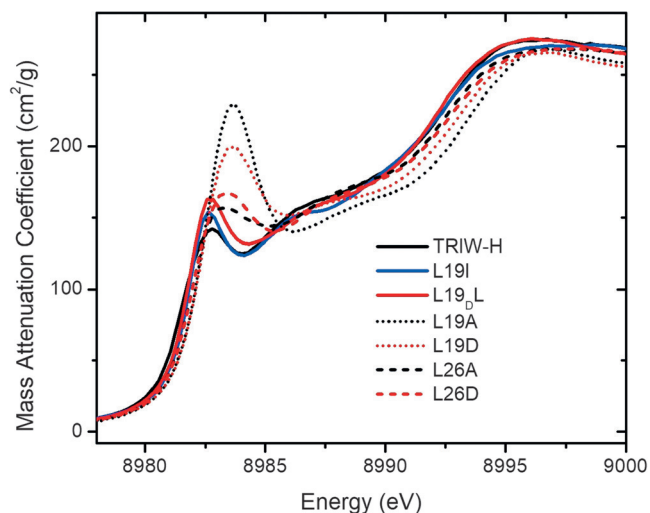


Figure 3. XANES of Cu^{I} bound constructs reported in this work, measured at pH 5.8.

While this decrease in coordination is not seen for L26A and L26D, all four constructs with enhanced NiR activity show an increase in the energy of the edge feature to 8983.6 ± 0.2 eV compared to 8982.8 ± 0.2 eV observed for TRIW-H. Exploring the EXAFS region (Supporting Information), we find two different categories of constructs based upon the Cu–N distance as well as number of imidazoles used in the model, which follow the categories defined by the XANES analysis. TRIW-H, L19I, L26A, and L26D are all best fit by a model utilizing three imidazoles at 1.91–1.93 Å with Debye–Waller values between 9.3 and $10.2 \times 10^{-3} \text{ \AA}^2$. Meanwhile, L19A and L19D make up the second category, fitting best with two imidazoles at 1.86–1.88 Å with Debye–Waller values of 8.0 or $7.8 \times 10^{-3} \text{ \AA}^2$, respectively (Table 2). The fitted Debye–Waller factors are somewhat larger than usual, suggesting that there is some disorder in these sites.

These structural observations indicate that the steric bulk in the second coordination sphere above the His₃ layer prevents Cu^{I} from adopting a linear geometry, thereby forcing the binding of an “extra” imidazole to Cu^{I} . Once this steric

Table 2: EXAFS fitting parameters and first order NiR kinetics of interior mutation constructs reported in this work compared to TRIW-H.^[6]

Construct	Model	Cu–NR [Å]	Cu–N $\sigma^2 \times 10^{-3}$ [Å ²]	Rate [s ⁻¹]
TRIW-H	3 Cu–His	1.93	ca. 9	4.6×10^{-4}
L19 _D L	3 Cu–His	1.92	9.8	9.7×10^{-4}
L19A	2 Cu–His	1.86	8.0	3.5×10^{-2}
L19D	2 Cu–His	1.88	7.8	2.4×10^{-2}
L26A	3 Cu–His	1.91	10.1	2.2×10^{-2}
L26D	3 Cu–His	1.91	8.6	3.4×10^{-2}

bulk is removed, as in the case of L19D and L19A, Cu^{I} readily adopts its preferred linear geometry, leaving an unbound imidazole. In previous studies with Hg^{II} , we demonstrated that providing three cysteine sulfurs that were predisposed for metal binding led to a higher than normal metal coordination environment [from $\text{Hg}^{\text{II}}(\text{SR})_2$ to $\text{Hg}^{\text{II}}(\text{SR})_3$].^[7,26,27] We have also explored how increased steric bulk in the layer above a Cd^{II} and a three Cys plane can decrease the coordination number of the cation [from $\text{Cd}^{\text{II}}(\text{SR})_3(\text{H}_2\text{O})$ to $\text{Cd}^{\text{II}}(\text{SR})_3$].^[17,28,29] The present system provides the first example in which enhancement of steric bulk in the second coordination sphere leads to an increase in the coordination number of the bound metal ion (from $\text{Cu}^{\text{I}}(\text{His})_2$ to $\text{Cu}^{\text{I}}(\text{His})_3$).

At this point, it is worth assessing why the L19A, L19D, L26A, or L26D peptides have such an increased NiR rate compared to all previously prepared 3SCC NiR mimics. As discussed above, increased substrate access is one possibility, though our observation that L19I, with greater steric bulk, does not exhibit a decreased rate relative to TRIW-H leaves this uncertain. It would be tempting to conclude that the enhanced NiR rates of the L19A and L19D constructs are a consequence of their two-coordinate nature, but in this case, one would expect that neither L26A or L26D would show enhanced NiR reaction rates. One striking commonality between all the constructs presented with enhanced NiR activity, is the approximate 1 eV shift observed in the XANES edge feature. This shift is greater in the two-coordinate constructs but is observed in all four enhanced activity constructs. Previous work has shown that both coordination number and geometry can affect the energy of the $1s \rightarrow 4p$ transition, where an increase in $4s-4p$ mixing results both in a decrease in intensity and shift to lower energy, which may already account for the differences seen in Figure 3.^[25] Another possibility is that small changes in the 3SCC bundle may affect the net electron density on the bound Cu^{I} which leads to an energy shift of the edge. This last explanation is particularly intriguing as it provides a plausible explanation as to how constructs with three- or two-coordinate Cu^{I} could have similarly enhanced NiR rates. The change in the net charge of the bound Cu would then lead to similarly increased rates of nitrite reduction amongst all four constructs.

In summary, steric bulk above the histidine layer has been used to enforce a non-preferred metal coordination geometry in TRIW-H, L19I, and L19_DL, providing a novel strategy for the incorporation of desired metal coordination in metalloproteins. The substitution of Leu to Ala or Asp at the 19th or 26th positions of TRIW-H leads to a 45–75-fold increase in NiR activity with a catalytic efficiency of $1.0(0.3) \text{ s}^{-1} \text{ M}^{-1}$ at pH 5.8 for L19A. The cause for this increase in NiR activity is still under investigation, but XANES gives evidence that this enhancement is likely significant for the Cu^{I} species, with all increased rate constructs showing a similar 1 eV shift in their edge transition energies. This shift may be caused by geometric or electrostatic changes, and this will require further investigation. It should be noted that L19A, L19D, L26A, and L26D could differ structurally in the Cu^{I} state in the absence of substrate, while all constructs may ligate three His once nitrite binds as we have previously shown with CO binding to

these constructs.^[30,31] Future designs will attempt to distinguish between these two possible effects and will provide guidance for NiR models with even higher catalytic efficiency.

Acknowledgements

V.L.P. thanks the National Institutes of Health for financial support of this research (ES012236). We thank Dr. Leela Ruckthong and Dr. Tyler Pinter for the helpful comments and discussion.

Conflict of interest

The authors declare no conflict of interest.

Keywords: copper nitrite reductase · de novo design · second coordination sphere · steric properties · TRI peptide

How to cite: *Angew. Chem. Int. Ed.* **2018**, *57*, 3954–3957
Angew. Chem. **2018**, *130*, 4018–4021

- [1] F. Yu, V. M. Cangelosi, M. L. Zastrow, M. Tegoni, J. S. Plegaria, A. G. Tebo, C. S. Mocny, L. Ruckthong, H. Qayyum, V. L. Pecoraro, *Chem. Rev.* **2014**, *114*, 3495–3578.
- [2] C. S. Mocny, V. L. Pecoraro, *Acc. Chem. Res.* **2015**, *48*, 2388–2396.
- [3] W. F. DeGrado, C. M. Summa, V. Pavone, F. Nastro, A. Lombardi, *Annu. Rev. Biochem.* **1999**, *68*, 779–819.
- [4] M. L. Zastrow, A. F. A. Peacock, J. A. Stuckey, V. L. Pecoraro, *Nat. Chem.* **2012**, *4*, 118–123.
- [5] M. L. Zastrow, V. L. Pecoraro, *J. Am. Chem. Soc.* **2013**, *135*, 5895–5903.
- [6] M. Tegoni, F. Yu, M. Bersellini, J. E. Penner-Hahn, V. L. Pecoraro, *Proc. Natl. Acad. Sci. USA* **2012**, *109*, 21234–21239.
- [7] G. R. Dieckmann, D. K. McRorie, J. D. Lear, K. A. Sharp, W. F. DeGrado, V. L. Pecoraro, *J. Mol. Biol.* **1998**, *280*, 897–912.
- [8] H. J. Wijma, L. J. C. Jeuken, M. P. Verbeet, F. A. Armstrong, G. W. Canters, *J. Biol. Chem.* **2006**, *281*, 16340–16346.
- [9] C. B. Bell, J. R. Calhoun, E. Bobyr, P.-p. Wei, B. Hedman, K. O. Hodgson, W. F. DeGrado, E. I. Solomon, *Biochemistry* **2009**, *48*, 59–73.
- [10] A. J. Reig, M. M. Pires, R. A. Snyder, Y. Wu, H. Jo, D. W. Kulp, S. E. Butch, J. R. Calhoun, T. G. Szyperski, E. I. Solomon, W. F. DeGrado, *Nat. Chem.* **2012**, *4*, 900–906.
- [11] A. Roy, I. Sarrou, M. D. Vaughn, A. V. Astashkin, G. Ghirlanda, *Biochemistry* **2013**, *52*, 7586–7594.
- [12] A. Roy, D. J. Sommer, R. A. Schmitz, C. L. Brown, D. Gust, A. Astashkin, G. Ghirlanda, *J. Am. Chem. Soc.* **2014**, *136*, 17343–17349.
- [13] W. Kaim, J. Rall, *Angew. Chem. Int. Ed. Engl.* **1996**, *35*, 43–60; *Angew. Chem.* **1996**, *108*, 47–64.
- [14] I. S. MacPherson, M. E. P. Murphy, *Cell. Mol. Life Sci.* **2007**, *64*, 2887–2899.
- [15] F. Yu, J. E. Penner-Hahn, V. L. Pecoraro, *J. Am. Chem. Soc.* **2013**, *135*, 18096–18107.
- [16] M. E. P. Murphy, S. Turley, E. T. Adman, *J. Biol. Chem.* **1997**, *272*, 28455–28460.
- [17] A. F. A. Peacock, O. Iranzo, V. L. Pecoraro, *Dalton Trans.* **2009**, 2271–2280.
- [18] L. Ruckthong, A. F. A. Peacock, C. E. Pascoe, L. Hemmingsen, J. A. Stuckey, V. L. Pecoraro, *Chem. Eur. J.* **2017**, *23*, 8232–8243.
- [19] L. Ruckthong, A. Deb, L. Hemmingsen, J. E. Penner-Hahn, V. L. Pecoraro, *J. Biol. Inorg. Chem.* **2017**, *23*, 123–135.
- [20] D. Ghosh, V. L. Pecoraro, *Inorg. Chem.* **2004**, *43*, 7902–7915.
- [21] L. Ruckthong, M. L. Zastrow, J. A. Stuckey, V. L. Pecoraro, *J. Am. Chem. Soc.* **2016**, *138*, 11979–11988.
- [22] L. Ruckthong, University of Michigan (Ann Arbor, MI), **2016**.
- [23] N. Isoda, H. Yokoyama, M. Nojiri, S. Suzuki, K. Yamaguchi, *Bioelectrochemistry* **2010**, *77*, 82–88.
- [24] N. J. Blackburn, R. W. Strange, J. Reedijk, A. Volbeda, A. Farooq, K. D. Karlin, J. Zubieta, *Inorg. Chem.* **1989**, *28*, 1349–1357.
- [25] L. S. Kau, D. J. Spira-Solomon, J. E. Penner-Hahn, K. O. Hodgson, E. I. Solomon, *J. Am. Chem. Soc.* **1987**, *109*, 6433–6442.
- [26] G. R. Dieckmann, D. K. McRorie, D. L. Tierney, L. M. Utschig, C. P. Singer, T. V. O'Halloran, J. E. Penner-Hahn, W. F. DeGrado, V. L. Pecoraro, *J. Am. Chem. Soc.* **1997**, *119*, 6195–6196.
- [27] B. T. Farrer, N. P. Harris, K. E. Balchus, V. L. Pecoraro, *Biochemistry* **2001**, *40*, 14696–14705.
- [28] O. Iranzo, C. Cabello, V. L. Pecoraro, *Angew. Chem. Int. Ed.* **2007**, *46*, 6688–6691; *Angew. Chem.* **2007**, *119*, 6808–6811.
- [29] A. F. A. Peacock, L. Hemmingsen, V. L. Pecoraro, *Proc. Natl. Acad. Sci. USA* **2008**, *105*, 16566–16571.
- [30] F. Yu, Ph.D. thesis, University of Michigan (Ann Arbor, MI), **2014**.
- [31] M. R. Ross, A. M. White, F. Yu, J. T. King, V. L. Pecoraro, K. J. Kubarych, *J. Am. Chem. Soc.* **2015**, *137*, 10164–10176.

Manuscript received: December 14, 2017

Accepted manuscript online: January 8, 2018

Version of record online: January 26, 2018